**Supplementary Information**

# Water-soluble Schiff base-actinyl ion complexes and their effect on the solvent extraction of *f*-elements

Cory A. Hawkins,*[a,b] Christian G. Bustillos,[a,c] Iain May,[c] Roy Copping,[c,d] and Mikael Nilsson[a]

[a] *University of California Irvine, Department of Chemical Engineering and Materials Science, Irvine, California 92617, USA.*

[b] *Current Address. Tennessee Technological University, Department of Chemistry, Cookeville, Tennessee 38506, USA. Tel: +1-931-372-6819; E-mail: cahawkins@tntech.edu*

[c] *Science, Technology and Engineering, Los Alamos National Laboratory, Los Alamos, New Mexico 87545, USA.*

[d] *Current Address. Isotope Development Group, Oak Ridge National Laboratory, Oak Ridge, Tennessee 37830, USA.*

# Experimental

### $^1$H NMR Spectroscopy

Proton NMR spectra were recorded using a Bruker GN500 (500 MHz, $^1$H) spectrometer, equipped with a BBO probe and employing pulse gradient sequences for water solvent suppression.[1] Due to the prevalence of water in most of these samples, the phenolic protons are not observable. The spectral width was maintained at 16 ppm centered at 4.9 ppm, unless otherwise noted.

NMR samples were prepared in a manner that mimics the conditions of the aqueous phase in the extraction systems. Samples for Schiff base $^1$H NMR titration by U(VI) were prepared by dissolving a known weight of the ligand disodium salt in solutions of $UO_2(NO_3)_2$ (0 M to 2 mM) with 0.1 M $KNO_3$ at pH 4 (adjusted using 0.1 M acetic acid). The weight of the ligand and the total volume were held constant such that the formal concentration of the ligand was 10 mM. To a 0.900 mL portion of these solutions, 0.100 mL of $D_2O$ (99.98%, Cambridge Isotope Labs, Tewksbury, MA, USA) was added and the solutions were allowed to equilibrate for at least one hour prior to acquiring the spectra. To avoid metal ion hydrolysis, solutions for NMR spectroscopy of Schiff bases in the absence and presence of Eu(III) were prepared by combining 0.25 mL of 0.02 M $H_2$salen$SO_3$ (pH adjusted to 5.5 with 0.1 M $HNO_3$) with 0.5 mL 0.2 M $KNO_3$ (pH adjusted to 5.5 by dilute acetic acid), a volume of 0.1 or 0.01 M $Eu(NO_3)_3$ stock, and 0.100 mL $D_2O$ with make-up DI water such that the final formal concentration of the Schiff base was 5 mM and the range of Eu(III) concentrations were from 0 M to 5.0 mM. Solution pH was measured by potentiometry.

Acid dissociation constants of the ligand were estimated through titration of a $H_2$salen$SO_3$ stock solution with either standardized 0.1 M $HNO_3$ or 0.1 M NaOH between pH 3 and 11.5 (initial pH of 7.89), measured by electrode. The final solutions contained 5.0 mM $H_2$salen$SO_3$ (formal concentration), 1.0 mM ammonium acetate (internal standard) and 10% (v/v) $D_2O$ in 0.1 M $KNO_3$. Proton NMR spectra of these samples were recorded and the equilibrium constants were calculated by nonlinear least-squares regression using the non-labile proton chemical shifts and the HypNMR computer program.[2]

### UV-vis Spectrophotometry

UV/Vis spectrophotometric titrations were designed to study the formation of U(VI) complexes with $H_2$salen$SO_3$ and 5-sulfonato-salicylaldehyde. An Olis-upgraded Cary 14 UV-vis-NIR spectrophotometer was used to collect spectra. The instrument is equipped with a thermostatic system to control the temperature of the solutions in both the sample and reference cells. Spectra were collected using quartz cells (1.00 cm path length, Hellma) in the wavelength region 250-600 nm at 1 nm increments and 3 points per datum, where absorbance by both the ligands, U(VI), and their complexes occurs. Prior to each

experiment, a baseline spectrum was collected using 0.1 M ammonium acetate buffer pH 5.5 in both the sample and reference cells. Then, batch titration solutions of $H_2$salen$SO_3$ (0.1 mM to 4.0 mM formal concentrations) with 0.75 mM $UO_2(NO_3)_3$ in 0.1 M ammonium acetate buffer pH 5.5 (to avoid pH excursions) with $KNO_3$ as the inert background electrolyte to maintain ionic strength at 0.1 M, were prepared and transferred to the sample cell for analysis at 25°C.

*Estimation of Aqueous U(VI)-Schiff Base Complex Stability Constant*

Data from titrations of U(VI) by $H_2$salen$SO_3$ using UV-visible spectrophotometry (450-600 nm) were imported into the HypSpec program as a composite file. The calculated protonation constants and all other pertinent equilibria were included in the model to estimate the stability constant of the $UO_2$-salen$SO_3$ complex in aqueous solution, under conditions that best represent the extraction system, while holding the pH nearly constant.

**Extractions of uranium, neptunium, curium, and europium**

The concentration of $UO_2^{2+}$ was chosen to provide sufficient count rates after neutron activation of the samples, while being much lower than the estimated formal concentration of the extractant and complexants. Specific activity of the $^{152/154}$Eu radiotracer was high enough to measure the distribution ratios, but maintain a low enough concentration of Eu(III) to avoid exceeding the metal cation capacity of the organic phase and mitigate the formation of polymeric species. At each timepoint, the phases were disengaged by centrifugation, equal volume aliquots of the phases were removed and 100 µL of each sampled in triplicate for analysis. Comparison of the extraction without a holdback reagent was carried out with a similar system (1 mL each phase) in the absence of a Schiff base and contacting for 30 min. The extent of extraction was calculated as a distribution ratio (ratio of the count rate in equilibrated organic phase to that in the aqueous phase). Mass balance recoveries (all between 94% and 111%) were determined by the ratio of the sum of count rates in both phases post-phase contact to the count rate for the metal ion-spiked aqueous solution used in the extraction.

Uranium samples for the $H_2$salen$SO_3$ system were transferred to 1.4 mL neutron activation analysis (NAA) polytubes (L&A plastic Molding, Yorba Linda, CA) and an 8 mL NAA polytube was used for secondary containing and was heat sealed as well. These samples were irradiated in the rotating sample rack of the UC Irvine Mark I TRIGA nuclear reactor for 1 hour at 250 kW (estimated neutron flux of $8 \times 10^{11}$ n $cm^{-2}$ $s^{-1}$). The $^{239}$U product ($t_{1/2}$ = 23.45 minutes) was allowed to decay, whereupon the $^{239}$Np ($t_{1/2}$ = 2.36 days) decay gamma rays were counted using a Canberra high purity germanium (HPGe) detector operated with GenieTM 2000 (v. 3.2.1) gamma acquisition and analysis software. Count rates were normalized to the reactor shutdown time and counting errors (2σ) were calculated by the software.

Neptunium-237 and curium-244 samples were dissolved in 3 mL liquid scintillation cocktail (Ready Safe™, Beckman-Coulter, Fullerton, CA) and counted using a Beckman-Coulter LS6500 scintillation system with a printer output. Prior to analysis, the $^{237}$Np samples were stored in the dark for at least 40 days to approach secular equilibrium with respect to the $^{233}$Pa daughter and then recounted at 820 days to establish equilibrium ($t_{max}$ = 670 days). Establishing this steady state cancels the effect of daughter in-growth on the distribution measurements and is an established method for counting $^{237}$Np in solvent extraction experiments.[3] Count rates from a manually set window of the spectrum (non-calibrated 0-350 keV for $^{137}$Np and 150-350 keV $^{244}$Cm), shown in Fig. S1, were used to calculate distribution ratios. The total count rates in the $^{137}$Np samples were used to calculate the Np distribution ratios. Alpha events from $^{244}$Cm were the only significant contribution to in the gated channel for the calculation of the Cm distribution ratios. Europium-152/154 samples were analyzed by directly counting the sample aliquots in polytubes using a Packard Cobra IITM series automatic gamma counter.

Overall uncertainties in the measurements were reported as the sum of the relative counting errors and standard deviations from triplicate samples at the 95% confidence interval. Except where noted, significant loss of metal ions from precipitation or other effects were not found, as mass balance recoveries for the extraction were generally 100 +/- 10%.

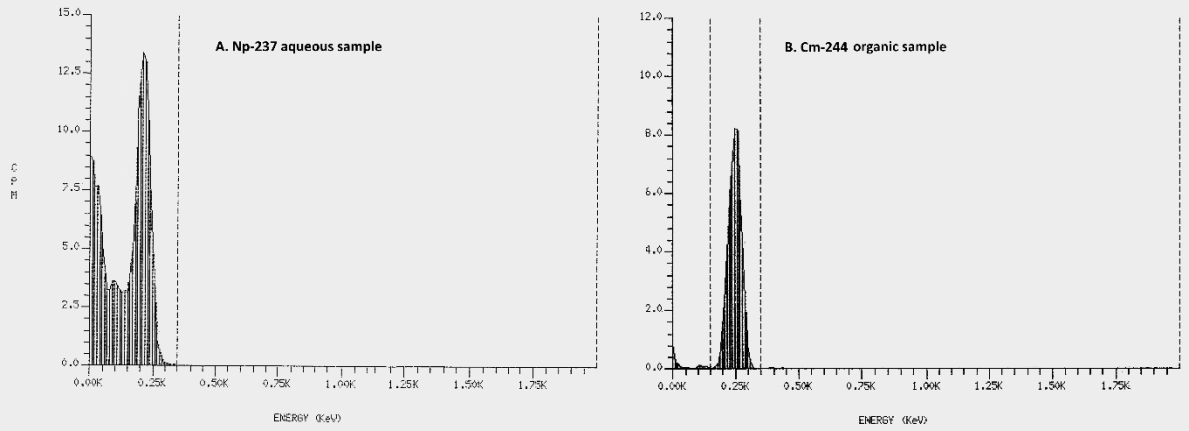


**Fig. S1**. Liquid scintillation raw spectra from counting of samples in the measurement of distribution ratios of A) Np-237 and B) Cm-244. Counting windows are indicated by the dotted lines.

## Results

### Np(V/VI)-$H_2$salen$SO_3$ complexation studies

In a first assessment of Np solution complexation with $H_2$salen$SO_3$, aqueous solutions of each reactant providing a 1:1 stoichiometry were combined and the pH was adjusted. An aliquot of a deep yellow 0.01 M aqueous solution of $H_2$salen$SO_3$ (120 uL, 1.2 mmol) in $H_2O$ was added to 50 uL of a previously prepared 0.024 M $^{237}$Np solution (1.2 mmol) in 1000 uL of $H_2O$ at a recorded pH of 2.56, at which the solution was colorless. The near-IR spectrum of this solution in Fig. S2 showed no evidence of complexation, as the intense absorption band at 980 nm is particular to the hydrated $NpO_2^+$ ion.[4-6] This spectrum also indicates that Np(VI) is not present, as the characteristic band near 1220 nm is absent. The pH was then raised to 10.0 with 100 uL of 1 M $NH_4OH$ and the solution turned yellow. A UV/Vis/nIR spectrum of the solution in Fig. S2 was collected showing evidence of full complexation by the red-shift of the Np(V) bands at 980 nm and 1024 nm to 996 nm and 1047 nm, respectively. Then, the pH was lowered to 9.05 with 1 M HCl and the appearance of the 980 nm band as a shoulder on the 996 nm band indicates that some decomplexation had occurred.

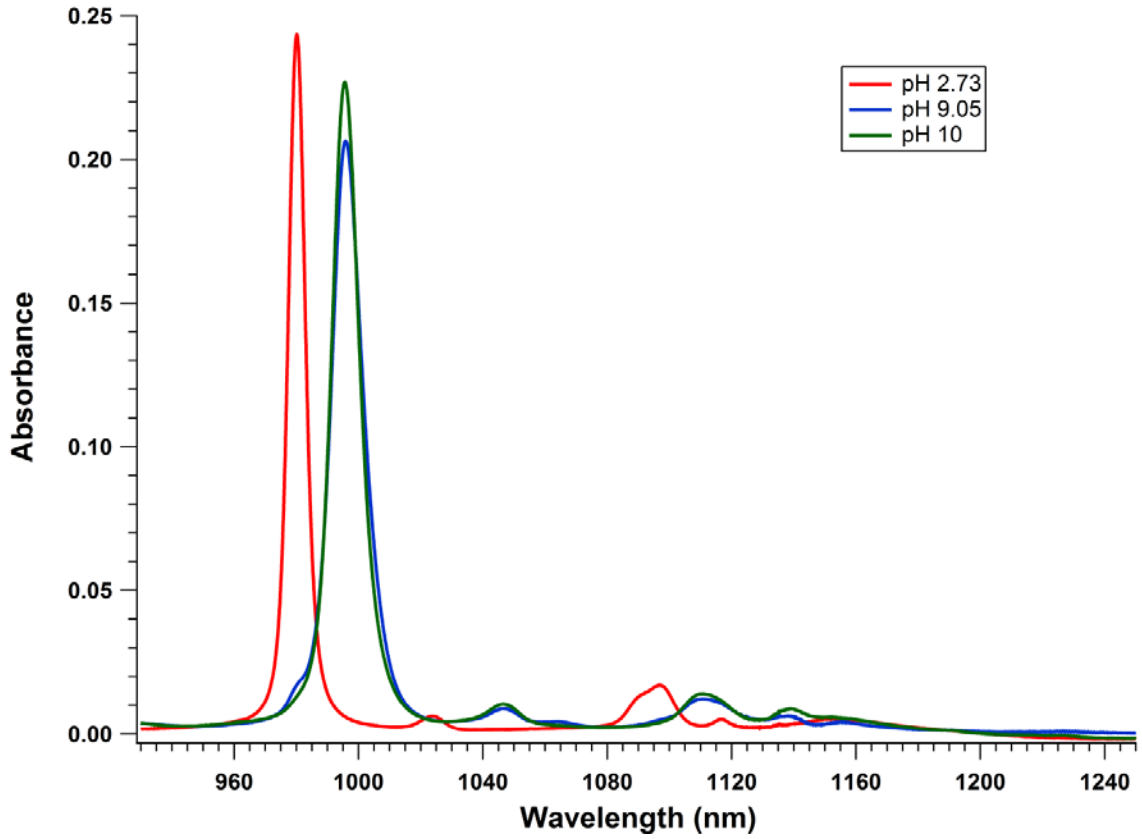


**Fig. S2**. Near-IR spectra of $NpO_2$(salen-$SO_3$) in water at pH 2.73, 9.05, and 10.0 (1 cm path length cell)

**Extraction data**

**Table S1.** Summary of extraction results: metal ion distribution ratios ($D_M$) and percent extraction (%*E*). Numbers in parentheses are the uncertainties from the combination of counting error and standard deviations of triplicate analysis at the 95% confidence interval.

| Timepoint (hours) | $D_U$ | $\%E_U$ | $D_{Np}$ | $\%E_{Np}$ | $D_{Eu}$ | $\%E_{Eu}$ | $D_{Cm}$ | $\%E_{Cm}$ |
|---|---|---|---|---|---|---|---|---|
| 0.25 | 0.13 (0.03) | 12% | 0.012 (0.005) | 1% | 1.9 (0.02) | 65.3% | 40 (7) | 97.6% |
| 0.5 | 0.13 (0.01) | 11% | 0.017 (0.001) | 2% | 3.9 (0.08) | 79.7% | 89 (24) | 98.9% |
| 1 | 0.17 (0.01) | 15% | 0.024 (0.006) | 2% | 28 (0.4) | 96.5% | 199 (64) | 99.5% |
| 1.5 | 0.21 (0.03) | 17% | 0.025 (0.003) | 2% | 44 (0.9) | 97.8% | 318 (69) | 99.7% |
| 2 | 0.41 (0.07) | 29% | 0.032 (0.002) | 3% | 61 (2) | 98.4% | 334 (113) | 99.7% |
| 3 | | | 0.036 (0.006) | 4% | 86 (3) | 98.9% | 637 (385) | 99.8% |
| 5 | 1.34 (0.2) | 57% | 0.055 (0.004) | 5% | 136 (8) | 99.3% | 1038 (912) | 99.9% |
| 10 | | | 0.086 (0.008) | 8% | 147 (6) | 99.3% | 1420 (971) | 99.9% |
| 24 | | | 0.184 (0.018) | 16% | 177 (10) | 99.4% | 1420 (1257) | 99.9% |
| 32 | 41 (23) | 98% | 0.213 (0.013) | 18% | 195 (13) | 99.5% | 2123 (1638) | 99.95% |
| 0.5, No $H_2$salen$SO_3$ | 98 (25) | 99% | 4.7 (0.7) | 83% | 19.9 (0.3) | 61% | 10 (2) | 91.3% |

**Protonation constants of $H_2$salen$SO_3$ estimated by $^1$H NMR**

From our previous work,[7] and the widely-reported mechanism of imine hydrolysis,[8] we were aware that partial hydrolysis of $H_2$salen$SO_3$ would occur in aqueous solution. However, from those data, the true extent of hydrolysis was unknown. Our approach to answer the question of the hydrolysis equilibrium and to elucidate the protonation constants of the ligand needed to estimate the U(VI) complex stability constant was a pH-metric titration using $^1$H NMR spectroscopy The experiments were carried-out under constant ionic strength (0.1 M) and 25ºC. Corriea *et al*. reported stepwise protonation constants (log β) of $H_2$salen$SO_3$ as 9.90 and 16.67, using a similar approach.[9] Interestingly, the constants for ethylenediamine (hydrolysis product) were reported as $pK_1$ = 6.77 and $pK_2$ = 9.90. This $pK_2$ is the same as the log $\beta_{101}$ reported for $H_2$salen$SO_3$ and the sum of both is exactly the same as the log $\beta_{102}$ reported for the Schiff base. Although these pK values are similar to those reported in partially aqueous media,[10] an investigation of the Schiff base protonic equilibria in solutions resembling that of the extraction aqueous phase was undertaken.

*Data in support of the $H_2$salen$SO_3$ protonation model*

A titration by $^1$H NMR spectroscopy was carried-out and the stacked plots of these spectra from pH 3.12 to pH 11.49 are provided in Fig. S3 and Fig. S4). After pH 10, significant alkaline-side hydrolysis is responsible for vanishing Schiff base signals. Using the acetate methyl resonance as an internal standard to quantify the amounts of the species in solution, *via* the azomethine protons (7, 7h) for Schiff base signals, the well-resolved B proton signal of the aldehyde, and the ethylene proton signal from ethylenediamine, the equilibrium distribution plot in Figure S5 was constructed. Trends in the overall distribution of the aldehyde and ethylenediamine account for the mass balance between the intact Schiff base and these hydrolysis products, and they resemble those reported previously for this compound.[10] Most notably, at the extraction pH of 5.5 (Fig. 2), the intact ligand concentration was only approximately 0.15 mM and the U(VI) concentration was 0.1 mM. Thus, U(VI) is expected to be completely bound by the intact Schiff base in the initial aqueous phase of that solvent extraction system. Favorability for the forward reaction in Eqn. 1 implies that the complex with the di-Schiff base is very strong, even when it is fully protonated in the presence of the 10-fold to 40-fold more abundant mono-Schiff base and aldehyde. How strong of a complex is it? This is a question that these experiments were designed to answer.

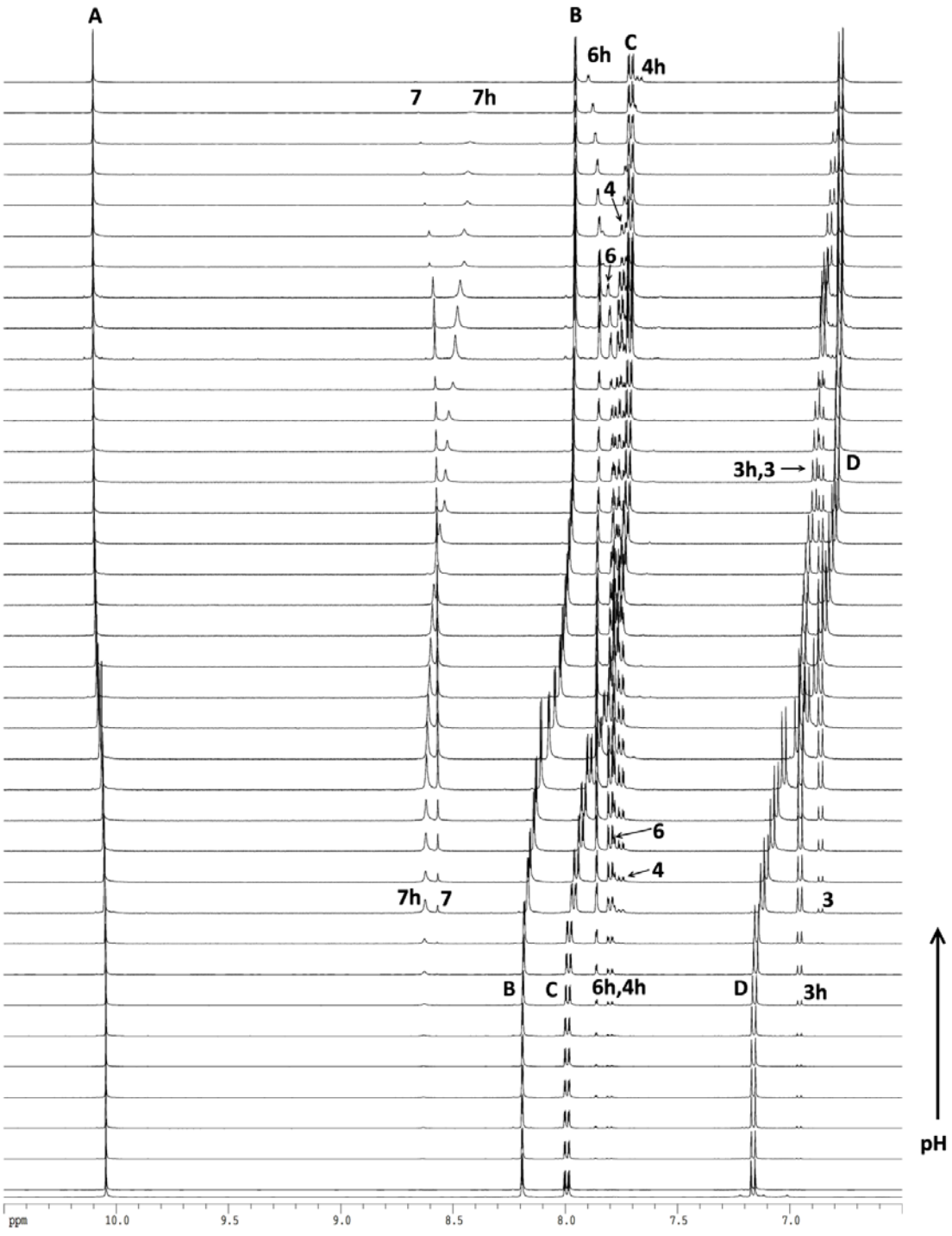


**Fig. S3.** Downfield proton NMR spectra from the titration of $H_2$salen$SO_3$ by 0.1 M $HNO_3$ or 0.1 M KOH from pH 3.12 to 11.49. The resonances are labeled according to the assignments made in Fig. 5 to indicate the change from initial to final states.

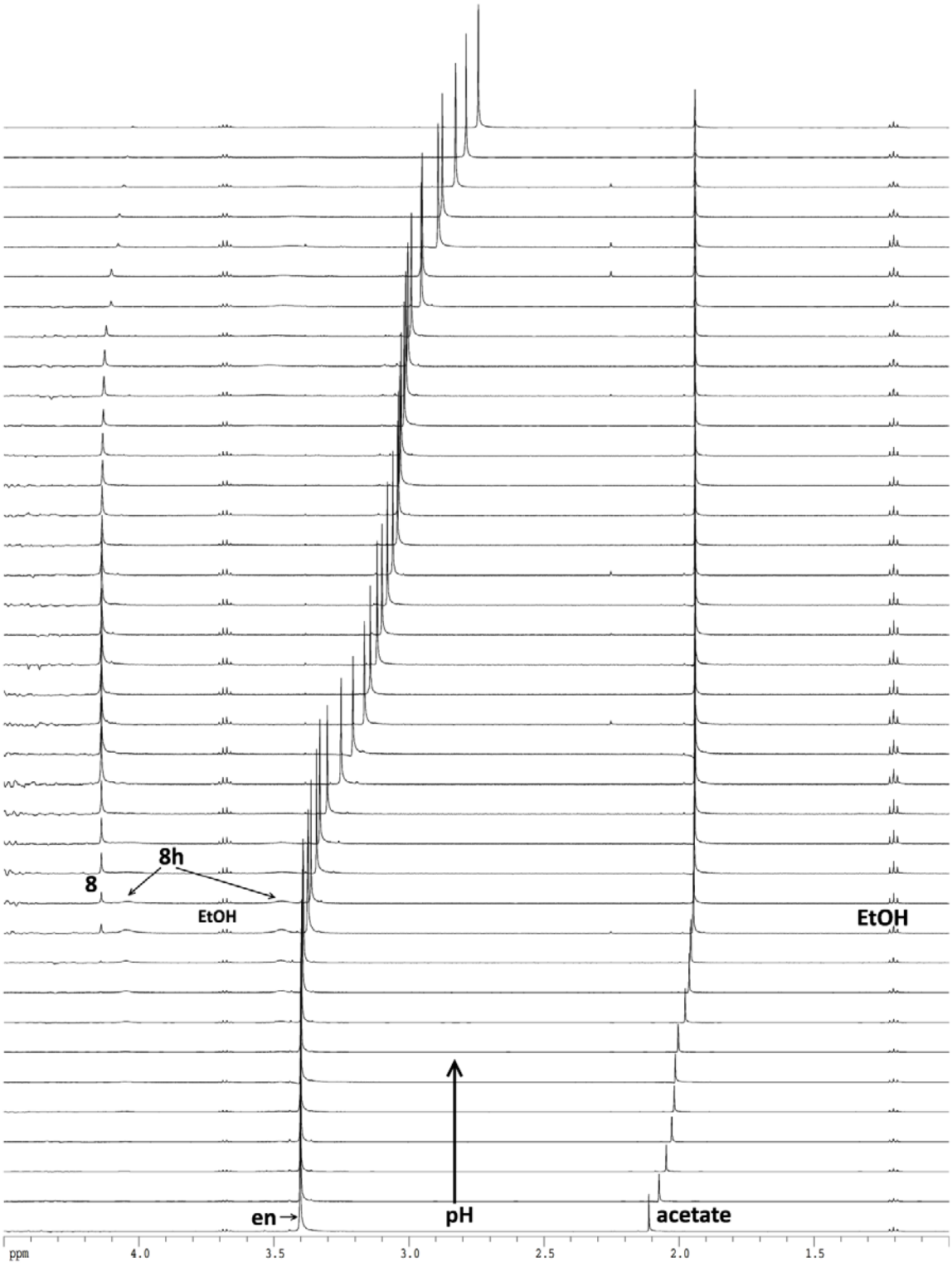


**Fig. S4.** Upfield proton NMR spectra from the titration of $H_2$salen$SO_3$ by 0.1 M $HNO_3$ or 0.1 M KOH from pH 3.12 to 11.49. The resonances are labeled according to the assignments made in Fig. 5 to indicate the change from initial to final states.

The pH distribution curve in Fig. S5 was compiled from these data. As expected, the mono-Schiff base (*i.e.*, partial hydrolysis product) is first to appear from the acid side and last to vanish on the alkaline side of the distribution curve (Fig. S5).

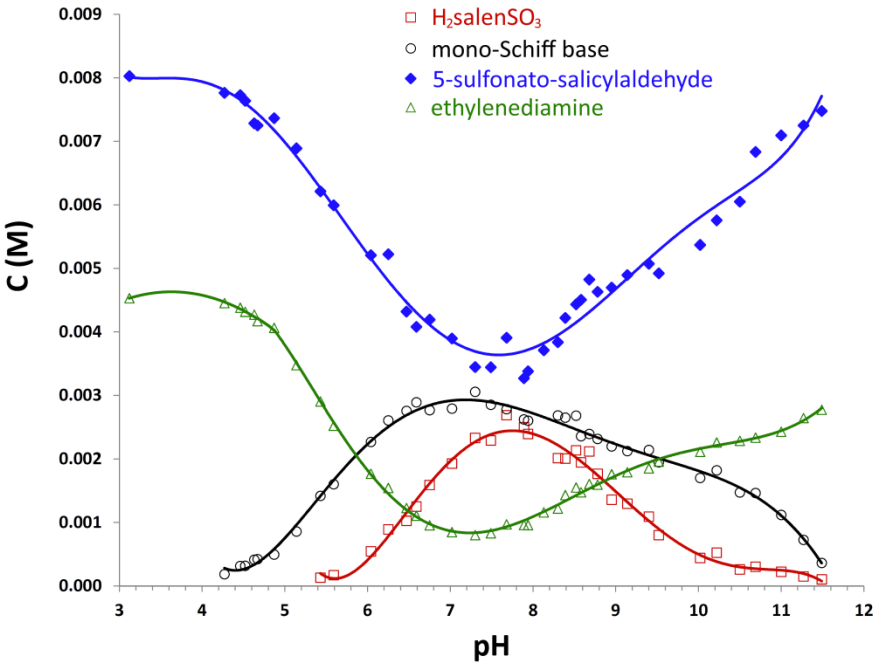


**Fig. S5.** Distribution of species with varying pH in solutions prepared at 5 mM (formal) $H_2salenSO_3$. Solutions comprising 0.1 M $KNO_3$, 1 mM ammonium acetate internal standard, and 10% $D_2O$ lock solvent were analyzed by proton NMR.

*Schiff base protonation model*

Subtle features of the distribution plot in Fig. 5 provide clues to overlapping equilibria of the di-Schiff base. Production of the di-Schiff base does not lead to a proportional reduction in the mono-Schiff base curve. Namely, a leveling-off of the mono-Schiff base (*i.e.*, partial hydrolysis product) concentration is observed between pH 8 and 10, indicating that a reaction was competing with hydrolysis in a region where the deprotonation of a Schiff base is expected. Accordingly, acid dissociation reactions were observed between pH 8 and 10 for the protons that are sensitive to the N-donors (protons 6 and 7) and O-donors (protons 3 and 4). The shift in these protons does not change in the range from pH 5 to 8, which is inconsistent with the previous report of an acid dissociation constant at 6.77.[9]

For the purpose of estimating metal ion-acidic ligand stability constants, the base proton interactions are conveniently written as proton association constants. Two protonation constants were found from the curves in the titrations shown in Fig. S6, one from the combination of protons 3 and 6 and the other from the combination of protons 4 and 7 (both N,O-donor combinations). The trends therein are consistent with the step-wise deprotonation of the N,O-donors for the two Schiff base moieties in $H_2salenSO_3$. Independent HypNMR calculations of these two sets of data result in stepwise protonations of log $\beta_{122}$ = 9.59 ± 0.09 and log $\beta_{121}$ = 19.6 ±0.1.

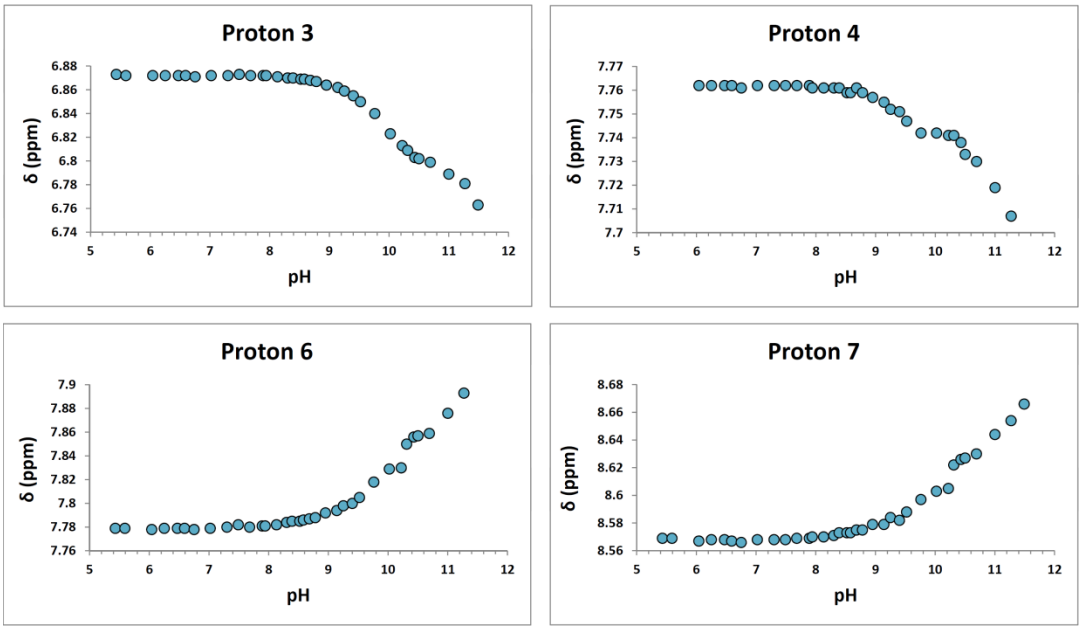


**Figure S6.** Plots of $^1$H NMR chemical shift (δ) for O-sensitive protons (3 and 4) and N-sensitive protons (6 and 7) versus pH in the strong acid-base titration of $H_2salenSO_3$ in solutions comprising 0.1 M $KNO_3$, 1 mM ammonium acetate, and 10% (v/v) $D_2O$.

In order to describe the close, two-step protic equilibrium, the Perrin model was employed, by which the extent of ionization between two dependent acid-base species is calculated using only spectroscopic data.[11,12] Recent studies accurately described the prototropic equilibria of a set of *ortho*-hydroxyaromatic Schiff bases using this technique, demonstrating a single protonation for a single N,O-donor system.[13,14] The mathematical model given in Equation 2 defines the quotient of the acidity constants $\Delta K_a$ for two acids HA and HB, which can be measured by the variation of the chemical shifts with changes in the acidity of the system.

$$\Delta K_a = \frac{K_a^{HA}}{K_a^{HB}} = \frac{[A][HB]}{[HA][B]} \qquad (2)$$

Conveniently, the sigmoid form of the functions with respect to chemical shift can be evaluated with the linear relationship in Equation 3

$$(\delta_b - \delta_{B^\circ})(\delta_{HA} - \delta_a) = \Delta K_\alpha(\delta_a - \delta_{A^\circ})(\delta_{HB} - \delta_{B^\circ}) \qquad (3)$$

where the slope is the equilibrium quotient $\Delta K_\alpha$ and the observed chemical shift of the species, $\delta_a$ and $\delta_b$, are in between those of the initial states, $\delta_{A^\circ}$ and $\delta_{B^\circ}$, and the final states, $\delta_{HA}$ and $\delta_{HB}$. Calculation of the equilibrium quotient allows one to estimate the difference in free energy of the system, and therefore, the propensity of the labile proton toward either donor in the system by $\Delta\Delta G° = -RT \ln\Delta K$. A plot of the chemical shift data for protons 3 and 6 from $H_2$salen$SO_3$ in the form of Equation 3 is provided in Figure S7, along with the calculated data listed in Table S2. Chemical shifts of these non-labile hydrogens were the most sensitive to changes in equilibria. The quotient of the equilibrium constants for the Schiff base donors $K_{NH}$ and $K_{OH}$ is given as $\Delta K_{NHO}$, and is the slope of this line corresponding to the ratio of equilibrium constants in the prototropic tautomerism. Results of the linear regression finds that $\Delta K_{NHO} = 1.00 \pm 0.01$ for $H_2$salen$SO_3$ under these conditions, giving rise to a $\Delta\Delta G° = 0$, and indicating that the labile proton is not favored by either the N or O atoms. Furthermore, the shielding trend in the O-sensitive chemical shifts (protons 3 and 4) and deshielding trend in the N-sensitive chemical shifts (protons 6 and 7) are consistent with deprotonation of the phenol and protonation of the imine during the titration, and give way to similar 1,5-tautomeric equilibria for both Schiff base moieties. Combined with the equilibrium position of the protons, we propose the model for deprotonation in Scheme S1. While this model is a simplification of the reactions that occur in solution, it corresponds to the mirrored, stepwise protonation constants for the di-Schiff base.

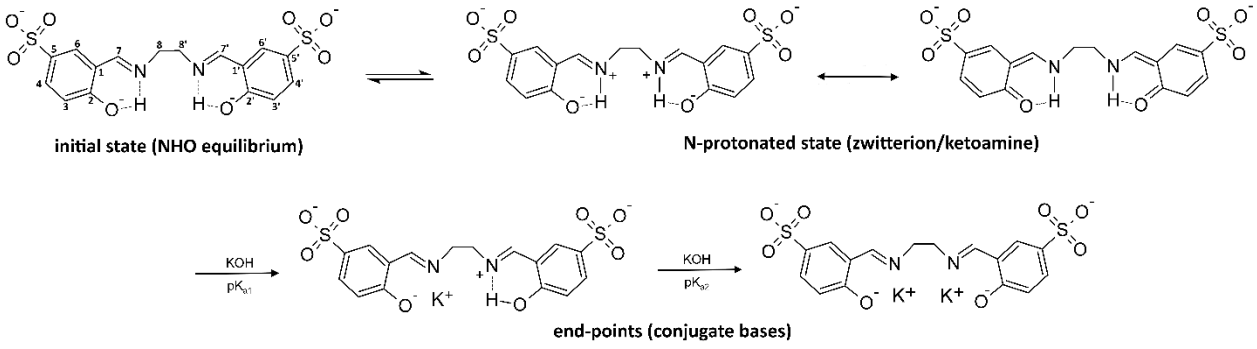


**Scheme S1.** Model for the prototropic equilibrium of $H_2$salen$SO_3$, during the strong base titration. The carbon number labels are the same as in Scheme 1. Carbon atoms are labeled according to the convention in Fig. 1 and the attached protons are referred to by these designations. The model is the simplest that fits the titration data and reports of salicylaldimine behavior and is not intended to represent exact structures in solution.

**Table S2.** Perrin model data for linear regression determination of $\Delta K_{NHO}$.

| pH | $\delta_6$ | $\delta_3$ | $(\delta_3-\delta_3^\circ)(\delta_6^e-\delta_6)$ | $(\delta_6-\delta_6^\circ)(\delta_3^e-\delta_3)$ |
|---|---|---|---|---|
| 8.3 | 7.784 | 6.871 | 0.000146 | 0.000345 |
| 8.39 | 7.785 | 6.87 | 0.000216 | 0.000408 |
| 8.58 | 7.786 | 6.869 | 0.000284 | 0.000469 |
| 8.68 | 7.787 | 6.868 | 0.00035 | 0.000528 |
| 8.78 | 7.788 | 6.867 | 0.000414 | 0.000585 |
| 8.95 | 7.792 | 6.864 | 0.000585 | 0.000806 |
| 9.14 | 7.794 | 6.862 | 0.000693 | 0.0009 |
| 9.25 | 7.798 | 6.858 | 0.000885 | 0.001064 |
| 9.4 | 7.801 | 6.855 | 0.001008 | 0.001166 |
| 9.52 | 7.805 | 6.852 | 0.001092 | 0.0013 |
| 9.76 | 7.818 | 6.84 | 0.001287 | 0.001482 |
| 10.02 | 7.829 | 6.83 | 0.001204 | 0.0014 |
| 10.22 | 7.845 | 6.815 | 0.000696 | 0.000858 |
| 10.31 | 7.85 | 6.811 | 0.000434 | 0.000639 |

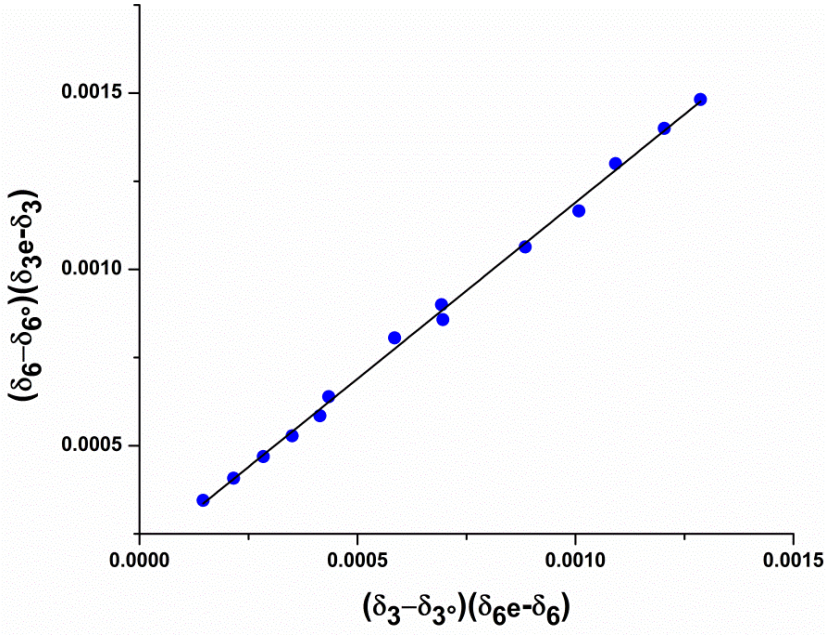


**Figure S7.** Perrin model plot using $^1$H NMR chemical shifts for N,O-sensitive protons of $H_2$salen$SO_3$ using the function in equation 3. The linear regression yields a line of y = 1.00(0.01)x + 0.0002(1E-5) with $R^2$ = 0.998.

**Aqueous $H_2salenSO_3$ hydrolysis states by $^1H$-$^1H$ COSY and NOESY**

The $^1H$ NMR spectrum of $H_2salenSO_3$ in water (Fig. 5) indicates two different species with imine groups. Investigation of the structural characteristics in this system was aided by two-dimensional proton NMR spectroscopy. COSY spectra of $H_2salenSO_3$ in aqueous solution alone and with nearly an equivalence of U(VI) are displayed in Fig. S8. The di-Schiff base azomethine resonance (7) has a strong correlation with the ethylene resonance (8) in panel A, where no methylene groups are observed for the mono-Schiff base. Formation of $[UO_2(salenSO_3)]^{2-}$ in a similar solution results in what appear to be long-distance correlations between the azomethine protons (7*) and two of the phenyl protons (3*and 6*). Such long-distance through bond correlations are consistent with aromatic resonance and symmetry in the ligand as a result of electronic orbital mixing by the LMCT of the complex. In fact, Schiff base *ortho*-hydroxy groups have been shown to form hydrogen bond bridges with adjacent imine groups, which leads to a coplanar conformation between these moieties.[13,14] Moreover, the stability of the six-membered ring created by such a bridge would lead to a significantly higher protonation constant for the Schiff bases than for that of the aldehyde. This difference is manifested in the difference between the phenolic proton dissociation constants calculated by HypNMR (mono-Schiff base $pK_a$ = 8.54 ± 0.01 and 5-sulfonato-salicylaldehyde $pK_a$ = 7.059 ± 0.008). Due to downfield shift of the ethylene proton frequency the resonance for this group in the complex is suppressed along with the water signal, eliminating its cross peaks.

NOESY experiments were performed on solutions of the of $H_2salenSO_3$ alone and saturated with U(VI), the spectra from which are presented in Fig. S9. Further verification of the Schiff base species assignments can be made from these data. Consistent with the nature of this through-space cross relaxation technique, the correlation of the azomethine (7h) and ethylene (8h) protons of the mono-Schiff base can be distinguished from those of the di-Schiff base (7 and 8). As expected, the 6*-7* and 3*-4* resonances of the complex are the only other protons coupled.

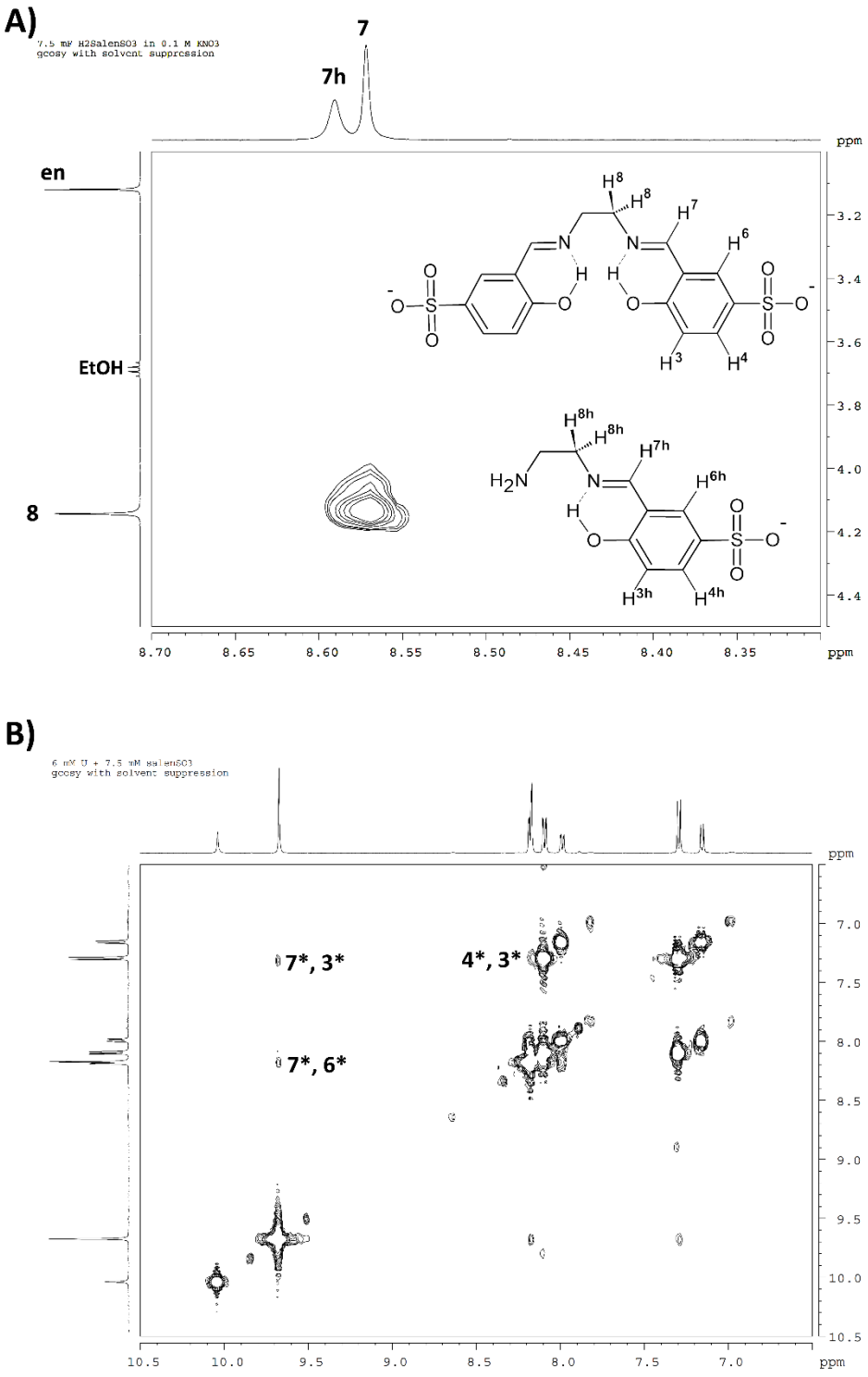


**Fig. S8.** $^{1}H$-$^{1}H$ COSY spectra of (A) 7.5 mF $H_2salenSO_3$ in 0.1 M $KNO_3$ alone and (B) in 0.1 M $KNO_3$ with 6 mM U(VI). The proton labels are provided for one-half the di-Schiff base molecule according to the carbon assignments made in Figure 1.

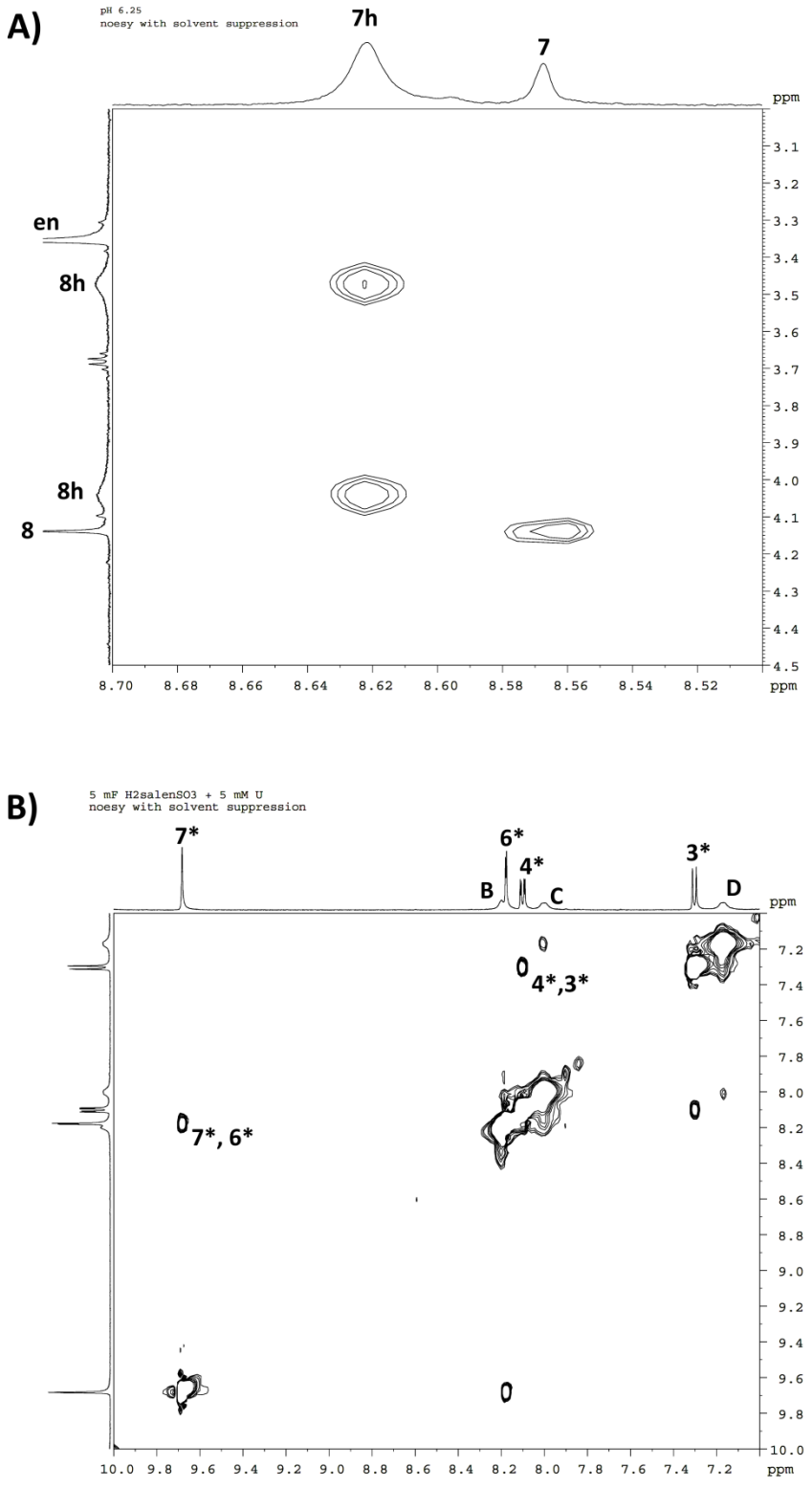


**Fig. S9.** NOESY spectra of (A) 5 mF $H_2$salen$SO_3$ in 0.1 M $KNO_3$ alone and (B) in 0.1 M $KNO_3$ with 5 mM U(VI). The resonance annotations are according to the assignments made in Figure 5.

**Lanthanide ion complexation in solution with $H_2salenSO_3$**

Neither UV-visible or $^1H$ NMR spectroscopy were successful in detecting significant complexation of La(III), Eu(III), or Nd(III) by $H_2salenSO_3$ or the mono-Schiff base in the presence of the aldehyde. However, lutetium is a smaller diamagnetic analog of europium, and can therefore be used as a probe to gauge how a decrease in lanthanide ion size will affect complexation without the introduction of paramagnetic shifts. Fig. S12 shows a series of $^1H$ NMR spectra with varying concentrations of Lu(III). Broadening of the aldehyde proton resonance and that for the proton adjacent to the alcohol is consistent with the results of Eu(III) and indicates that complexation with 5-sulfonyl-salicylaldehyde involves these O-donor groups. Along with noticeable aldehyde complexation with the addition of $Lu(NO_3)_3$ to a solution of $H_2salenSO_3$, there is noticeable peak splitting in the azomethine and ethylene bridge proton resonances of the di-Schiff base, which is consistent with the formation of a weak complex with the more charge-dense diamagnetic lanthanide cation (see Figures S12 and S13 in supplementary information). However, in contrast to the Eu(III) results, a small portion of the $H_2salenSO_3$ resonances are split upfield (denoted by subscript "Lu"), which is in accord with weak complexation of the di-Schiff base with Lu(III). Further evidence that Lu(III) binds weakly with the di-Schiff base can be found in a similar upfield shift for the ethylene bridge protons ($8_{Lu}$), seen in Fig. S13. This plot provides a zoomed view of the azomethine region of the spectra, showing the in-growth of the complex as the Lu(III) concentration increases. Interestingly, there appears to be a limit to how much of the complex can be formed, because the free ligand signal (7) does not vanish as the complex signal ($7_{Lu}$) reaches a steady state with increasing amounts of Lu(III). Similar experiments with lanthanum, on the other hand, did not indicate binding with this larger trivalent ion. Formation of a weak complex between the smaller Lu(III) ion and $H_2salenSO_3$ suggests that the binding site of the Schiff base may pose steric restrictions to the spherical lanthanide(III) ions.

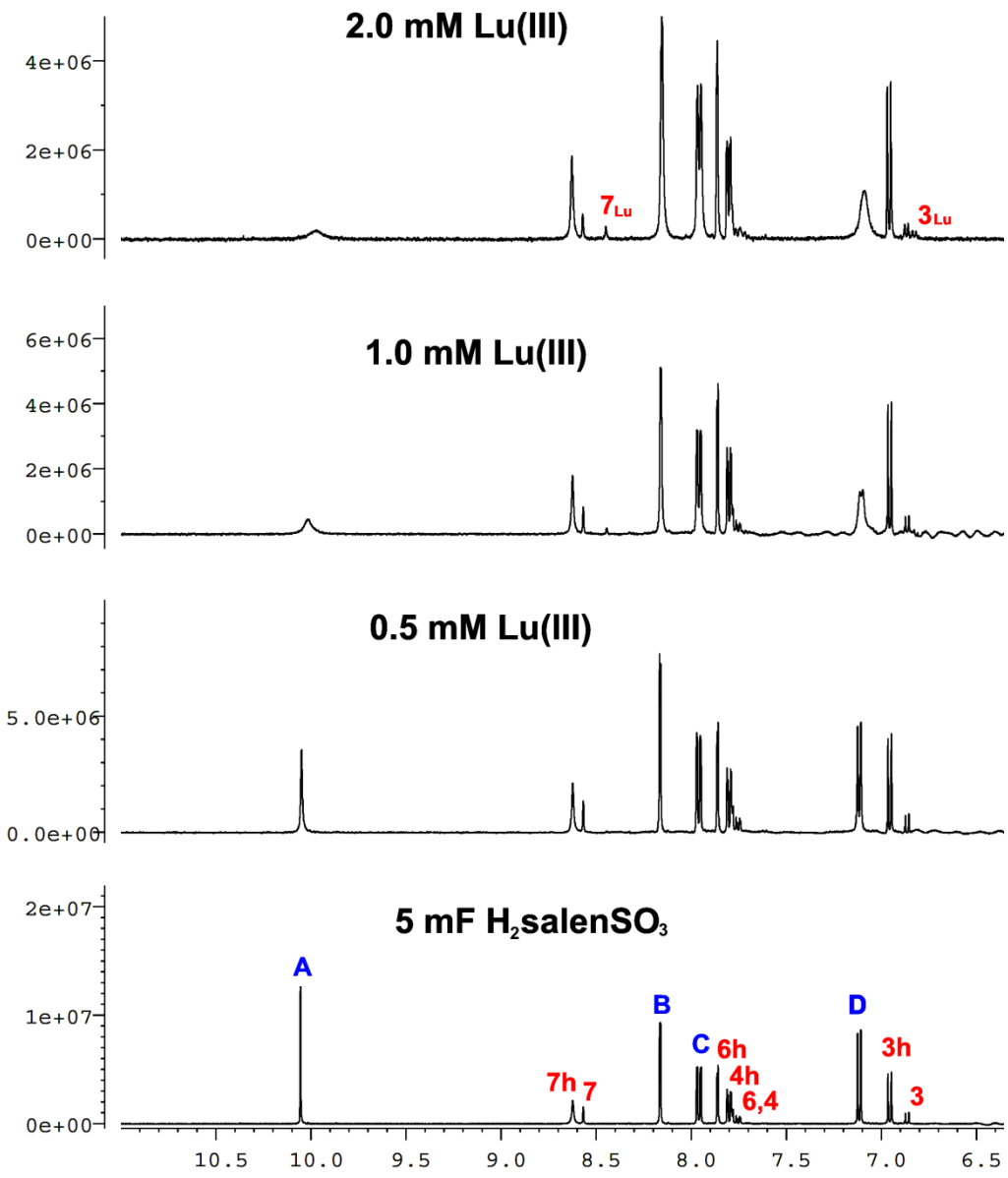


**Fig. S12**. Proton NMR spectra of 5 mF $H_2$salen$SO_3$ in 0.1 M $KNO_3$ (10% $D_2O$) in the absence and presence of varying concentrations of $Lu(NO_3)_3$. Annotations of the resonances follow the legend in Fig. 5. The subscript "Lu" designates the azomethine resonance shifted due to coordination with Lu(III).

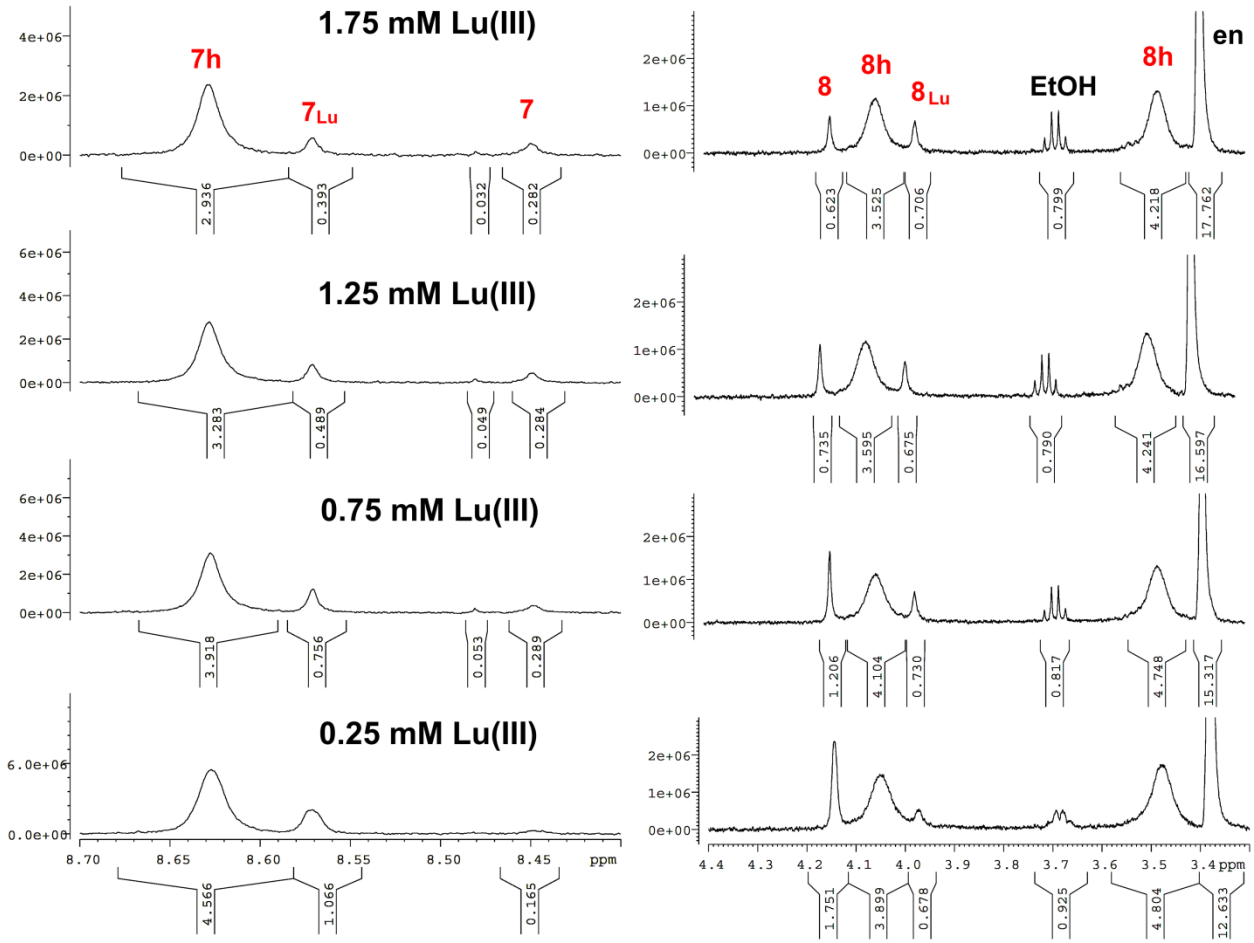


**Fig. S13**. $^{1}$H NMR spectra (downfield and upfield of the water signal) of 5 mF $H_2$salen$SO_3$ in 0.1 M $KNO_3$ (10% $D_2O$) in the absence and presence of varying concentrations of $Lu(NO_3)_3$. Annotations of the resonances follow the legend in Fig. S8(A). The subscript "Lu" designates the azomethine resonance shifted due to coordination with Lu(III).

**Estimation of $UO_2^{2+}$-Schiff base aqueous complex conditional stability constant**

UV-visible spectrophotometric investigations were undertaken to evaluate the U(VI)-salen$SO_3$ complex stability constant under conditions similar to the solvent extraction aqueous phase. In order to make these calculations, the extent of hydrolysis of $H_2$salen$SO_3$ in a sample prepared from the stock solution without uranium present was determined to be 52.5% by proton NMR. In the absence of the ammonium acetate buffer added to these samples, the ligand is the only buffering species. Therefore, to avoid significant hydrolysis and pH excursions, the buffer was added to all samples. Convergence of the model was tested by varying the estimated log β for the complex, which converged to 25.80 with estimates between 22 and 27. Compared to the results presented in Fig. S5 (50-fold decomposition), the acid hydrolysis reaction at

pH 5.5 was mitigated by the overall buffering capacity in these samples. Absorbance readings from these spectra in the 450 nm to 600 nm range were combined with the equilibrium constants in Table S3. The analysis is discussed in detail in the body of this paper.

**Table S3.** Equilibria involved in complexation under conditions similar to those of aqueous phase of solvent extraction system

| Reaction | log β [a] | Reference |
|---|---|---|
| $UO_2^{2+} + NO_3^- \rightleftharpoons UO_2NO_3^+$ | 0.62 ± 0.04 | [15] |
| $UO_2^{2+} + H_2O \rightleftharpoons UO_2OH^+ + H^+$ | -5.4 ± 0.24 | [16] |
| $2UO_2^{2+} + 2H_2O \rightleftharpoons (UO_2)_2(OH)_2^{2+} + 2H^+$ | -5.6 ± 0.02 | [16] |
| $3UO_2^{2+} + 5H_2O \rightleftharpoons (UO_2)_3(OH)_5^+ + 5H^+$ | -15.7 ± 0.02 | [16] |
| $H_2O \rightleftharpoons H^+ + OH^-$ | -13.78 | [17] |
| $CH_3COOH \rightleftharpoons CH_3COO^- + H^+$ | 4.76 ± 0.01 | [18] |
| $UO_2^{2+} + CH_3COO^- \rightleftharpoons UO_2(CH_3COO)^+$ | 2.68 | [18] |
| $UO_2^{2+} + 2CH_3COO^- \rightleftharpoons UO_2(CH_3COO)_2$ | 7.58 | [18] |
| $UO_2^{2+} + 3CH_3COO^- \rightleftharpoons UO_2(CH_3COO)_3^-$ | 13.88 | [18] |
| $HsalenSO_3^{3-} + H^+ \rightleftharpoons H_2salenSO_3^{2-}$ | 9.95 ± 0.09 | this work[b] |
| $salenSO_3^{4-} + H^+ \rightleftharpoons HsalenSO_3^{3-}$ | 19.59 ± 0.1 | this work[b] |
| $UO_2^{2+} + salenSO_3^{4-} \rightleftharpoons UO_2(salenSO_3)^{2-}$ | 25.80 ± 0.08 | this work[c] |

The uncertainty values for this work are presented are those obtained in the particular model shown.
[a] Equilibrium constants used for U(VI) nitrate and acetate complexation and U(VI) hydrolysis are those calculated for 0 M ionic strength at 25°C. [b] Ambient temperature (*ca*. 25 °C), ionic strength not fixed. [c] From UV-visible titration carried-out at 25 °C, ionic strength fixed.

*Assessment of aldehyde interference in UV-visible spectrophotometric experiments*

The effect of 5-sulfonato-salicylaldehyde on UV-visible spectroscopic studies was evaluated by collecting spectra of this compound in the absence and presence of uranyl nitrate under conditions similar to the titration with $H_2salenSO_3$. As can be seen in Figure S15, two n → π* transitions of the aldehyde produce bands centered about 325 nm and 370 nm. In contrast to the $H_2salenSO_3$ titration spectra, the interaction with U(VI) results in suppression of the band at 370 nm and small increases the band near 325 nm that are not just a simple sum of the absorbance of 0.75 mM U(VI) and the aldehyde. Most notably, the suppression of the 370 nm band in the presence or absence of U(VI) provides a region of the spectrum beginning at around 450 nm that generates minimal interference with the 460 nm LMCT of $H_2salenSO_3$, permitting the

measurement of the $[UO_2(salenSO_3)]^{2-}$ complex. Nonetheless, the 0.05 increase in absorbance on the post-equivalence plateau of the mole-ratio plot in Fig. 10 can be attributed to the non-zero baseline in that region of these spectra.

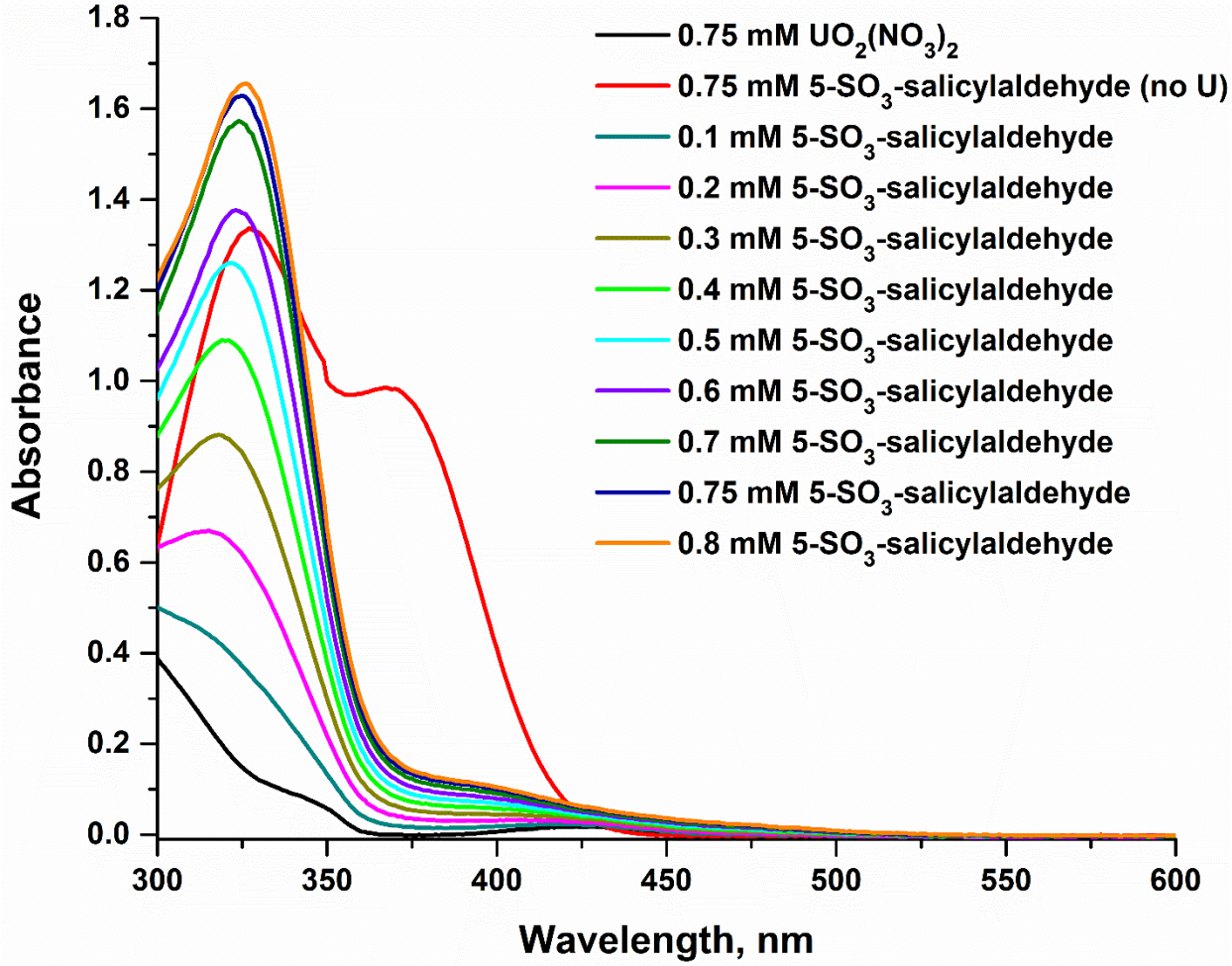


**Figure S14.** UV-visible spectra of varying concentrations of 5-sulfonato-salicylaldehyde in the absence and presence of 0.75 mM $UO_2(NO_3)_2$ in solutions prepared with 0.1 M $KNO_3$ and 0.05 M ammonium acetate buffer (pH 5.5). The arrow indicates increasing absorbance of the LMCT with increasing ligand concentration. Spectra of ligand and metal ion solutions alone are provided for perspective.

**References**


1. T. Hwang, A.J. Shaka, *J. Mag. Reson.* A, 112(2), 275-279, 1995.
2. P. Gans, A. Sabatini and A. Vacca, *Talanta*, 1996, **43**, 1739-1753.
3. E. Aneheim , C. Ekberg , A. Fermvik , M. R. St. J. Foreman , T. Retegan, G. Skarnemark, *Solv. Extr. Ion Exch.*, 2010, **28**, 437-458.
4. Z. Yoshida, S.G. Johnson, T. Kimura, J.R. Krsul, Neptunium. In *The Chemistry of the Actinide and Transactinide Elements*. L. Morss, N. Edelstein and J. Fuger, Eds. Springer: Netherlands, 763-765.
5. J.L. Ryan, Absorption spectra of actinide compounds. In *Lanthanides and Actinides*, *Inorganic Chemistry Series One*, Vol. 7; K.W. Bagnall, Ed.; Butterworths: London, 1972, 323-367.
6. R. Sjoblom, J.C. Hindman, *J. Am. Chem. Soc*. 1951. **73**, 1744-1751.
7. C.A. Hawkins, C.G. Bustillos, R. Copping, I. May, M. Nilsson, *Chem. Commun*., 2014, **50**, 8670-8673.
8. E. H. Cordes, W. P. Jencks, *J. Am. Chem. Soc*., 1962, **84**, 832–837.
9. I. Correia, J.C. Pessoa, M.T. Duarte, M. Fátima M. da Piedade, T. Jackush, T. Kiss, M. Margarida C. A. Castro, C.F.G.C. Geraldes, F. Avecilla, *Eur. J. Inorg. Chem*. 2005, 732–744.
10. D. Ortegón-Reyn, C. Garcías-Morales, I. Padilla-Martínez, E. García-Báez, A. Aríza-Castolo, A. Peraza-Campos, F. Martínez-Martínez, *Molecules*, 2014, **19**, 459-481.
11. C.L. Perrin, J.D. Thoburn, *J. Am. Chem. Soc*., 1989, **111**, 8010-8012.
12. C.L. Perrin, M.A. Fabian, *Anal. Chem*., 1996, **68**, 2127-2134.
13. S. Bilge, Z. Kiliç, Z. Hayvali, T. Hökelek, S. Safran, *J. Chem. Sci*., 2009, **121**, 989-1001.
14. A. Makal, W. Schilf, B. Kamieński,b, A. Szady-Chelmieniecka, E. Grech, K.Woźniak, *Dalton Trans*., 2011, **40**, 421–430.
15. L. Rao, G. Tian, *J. Chem. Thermodynamics*, 2008, **40**, 1001–1006.
16. P. Zanonato, P. Di Bernardo, A. Bismondo, G. Liu, X. Chen, L Rao, *J. Am. Chem. Soc*., 2004, **126**, 5515-5522.
17. R.F. Jameson M.F. Wilson, *J. Chem. Soc., Dalton Trans*., 1972, 2607-2610.
18. A. E. Martell and R. M. Smith, *Critical Stability Constants*, Vol. 3, Plenum, New York, USA, 1977; First suppl., 1982; Second suppl., 1989.